Car−Parrinello Molecular Dynamics Simulation of Fe^{3+}(aq)

Sami Amira,[†] Daniel Spångberg,[†,‡] Viktor Zelin,[†] Michael Probst,[‡] and Kersti Hermansson*[,†]

Materials Chemistry, The Ångström Laboratory, Uppsala University, Box 538, S-751 21 Uppsala, Sweden, and Institut für Ionenphysik, Leopold Franzens Universität, Technikerstrasse 25, A-6020 Innsbruck, Austria

Received: January 11, 2005; In Final Form: March 13, 2005

The optimized geometry and energetic properties of $Fe(D_2O)_n^{3+}$ clusters, with $n = 4$ and 6, have been studied with density-functional theory calculations and the BLYP functional, and the hydration of a single Fe^{3+} ion in a periodic box with 32 water molecules at room temperature has been studied with Car−Parrinello molecular dynamics and the same functional. We have compared the results from the CPMD simulation with classical MD simulations, using a flexible SPC-based water model and the same number of water molecules, to evaluate the relative strengths and weaknesses of the two MD methods. The classical MD simulations and the CPMD simulations both give Fe−water distances in good agreement with experiment, but for the intramolecular vibrations, the classical MD yields considerably better absolute frequencies and ion-induced frequency shifts. On the other hand, the CPMD method performs considerably better than the classical MD in describing the intramolecular geometry of the water molecule in the first hydration shell and the average first shell···second shell hydrogen-bond distance. Differences between the two methods are also found with respect to the second-shell water orientations. The effect of the small box size (32 vs 512 water molecules) was evaluated by comparing results from classical simulations using different box sizes; non-negligible effects are found for the ion−water distance and the tilt angles of the water molecules in the second hydration shell and for the O−D stretching vibrational frequencies of the water molecules in the first hydration shell.

1. Introduction

The chemical and physical properties of ions in aqueous solution are closely related to the structure and dynamics of the hydration shell (see, for example, ref 1 and references therein). Molecular Dynamics (MD) and Monte Carlo (MC) computer simulations have greatly helped to provide detailed microscopic information regarding the hydration shells around (metal) ions. Simulations have also been very helpful in interpreting experimental data from spectroscopic and diffraction experiments. However, many MD and MC simulations are based on two-body interaction potentials only, derived from ab initio calculations or fitted to experimental data. The inclusion of explicit higher-order terms, i.e., the many-body interactions in the potential energy expression, is not a trivial task and the potential energy expansion used in computer simulations is usually limited to the two- and three-body terms or to many-body polarization models. The many-body interactions are especially significant with *poly*valent ions in aqueous solution.

In recent years it has become possible to study aqueous solutions with the Car−Parrinello method (CPMD),[2] one of the most popular ab initio MD approaches. Instead of using an analytical force-field as in classical MD simulations, the forces acting on the particles in CPMD are obtained, at each time step, from first-principles electronic structure calculations, using Density Functional Theory (DFT) and a scheme that propagates both the nuclear and the electronic degrees of freedom simultaneously. One of the advantages of this method in the study of metal ion solvation is the natural inclusion of the many-body interactions. Another advantage (not used here) is that the Car−Parrinello MD method gives access to the electronic properties of the liquid. Unfortunately, the high computational cost of quantum-mechanical calculations usually limits the number of water molecules to 50−100 for simulation times longer than some 10 ps. Car−Parrinello simulations have been published for several metal ions in aqueous solution, namely Li^+,[3] Be^{2+},[4] Na^+,[5−7] Mg^{2+},[8] Al^{3+},[9] K^+,[10] Ca^{2+},[11] Fe^{2+},[12,13] Cu^{2+},[14] and Ag^+,[6] with varying degrees of success. CPMD simulations of anions in aqueous solution have also been published (see, for example, the study of Raugei and Klein[15] of the bromide ion solvation shell).

The ferric ion in aqueous solution has been the subject of several previous classical computer simulations (MD, MC) in the literature with the emphasis on solvation-shell structure,[16−22] ion and water diffusion,[21,22] hydrolysis,[23] charge transfer,[24−29] and solvent isotope effects.[18,19] Moreover, QM/MM-MD simulations of Fe^{3+}(aq) were recently reported[30,31] and structural properties, diffusion, and the librational and vibrational motion of the water molecules around Fe^{3+} were presented. A number of quantum-mechanical $Fe(H_2O)_n^{3+}$ cluster studies, including the work of Curtiss et al.[32] and Chang and Wang,[33] have been reported.

In this paper we present a Car−Parrinello simulation of a single Fe^{3+} ion in a periodic box of 32 water molecules. Structural and vibrational properties have been calculated from the CPMD trajectories. The CPMD simulation time (7 ps after equilibration) is too short for a reliable calculation of dynamical properties such as diffusion coefficients and residence times; thus such quantities are not presented here. The aim of the present study is to investigate the hydration shell structure and water vibrations for the hydrated ferric ion.

* To whom correspondence should be addressed. E-mail: kersti@mkem.uu.se.
[†] Uppsala University.
[‡] Leopold Franzens Universität.

10.1021/jp050186u CCC: $30.25
Published on Web 07/02/2005

TABLE 1: Overview of the Systems Studied and the Methods Used for Each System[a]

system	QC	CPMD	CLMD
D_2O(g)	1	1	1
D_2O(l)		32	32
$Fe(D_2O)_n^{3+}$(g)	4, 6	4, 6	
Fe^{3+}(aq)		32	32, 512

[a] The table lists the number of water molecules included (always one cation). CPMD and CLMD refer to the Car−Parrinello and classical MD simulations, respectively (see text for details). The QC column refers to quantum-mechanical cluster calculations with geometry optimization using the BLYP functional and the 6-31G** basis set.

We compare the results of the CPMD simulations with classical MD simulations to help evaluate the strengths and weaknesses of the CPMD simulation results. For the classical MD simulation, we use the same system size as in the CPMD simulations and a force-field known to describe the hydration structure and dynamics around Fe^{3+} rather well. Moreover, to assess the influence of the choice of system size, we have performed the classical MD simulations both with a box of the same size as in the CPMD simulations, as mentioned, and with a larger simulation box (512 water molecules).

Prior to the CPMD investigation, we have undertaken a comparative plane-wave versus local basis-set study to help assess the quality of the plane-wave cutoff and the pseudopotential used in the CPMD simulations. For this purpose, the interaction energies, the ion−water distances, and the internal water geometries were computed for $Fe(D_2O)_4^{3+}$ and $Fe(D_2O)_6^{3+}$ clusters, using the two approaches.

The outline of this paper is as follows. The CPMD simulation and the classical MD simulations are described in the Method section. The results and discussion section contains a presentation of the ab initio results for the $Fe^{3+}(D_2O)_n$ clusters, followed by the structural and OD stretching vibrational properties calculated from the different MD simulations. Our conclusions are given in the last section.

2. Method

The various systems studied and the different methods used are summarized in Table 1. Details of the different systems and methods are given below.

2.1. CPMD Simulations. We performed the Car−Parrinello simulations for a system consisting of 32 water (D_2O) molecules and one Fe^{3+} ion in a periodic cubic box of 10.16 Å side length, corresponding to a light-water density of 1.000 g/cm^3. The electronic structure of the valence electrons was described by DFT, using the BLYP functional, where the exchange functional is given by Becke[34] and the correlation energy expression by Lee, Yang, and Parr.[35] The valence electron wave function was expanded in plane waves with an energy cutoff at 60 Ry.

For the core electrons of the oxygen and hydrogen atoms, we have used the ultrasoft (US) pseudo-potentials developed by Vanderbilt.[36] For the ferric ion, we have also used the ultrasoft pseudo-potentials by Vanderbilt,[36] with an improved description of the core region using the nonlinear core correction (NLCC).[37] This correction is particularly appropriate in the case of transition metal ions.

All the CPMD simulations were done with the program package CPMD[38] in the NVT ensemble, with the pseudo-Hamiltonian being conserved within 10^{-4} au/ps. The initial configuration was taken from an equilibrated classical MD simulation of a single Fe^{3+} ion in a solution of 32 water molecules at 298 K, as described below. The Car−Parrinello system was first equilibrated for 3 ps, followed by 7 ps of data collection. The time step was 0.16 fs and the effective electron mass was 900 au. The hydrogen nuclei were treated as classical particles with the mass of the deuterium isotope, which allowed us to use this larger time step.[39] The temperature was kept around 300 K, using a Nosé-Hoover chain of thermostats.[40] The Nosé-Hoover chain of thermostats[40] was also applied to the electronic degrees of freedom. A homogeneous background charge was applied to compensate for the ionic charge. These simulations will be referred to as *CPMD-32* in the following.

As a reference, we have also performed a CPMD simulation of pure liquid water with 32 D_2O molecules in a periodic cubic box of 9.87 Å side length (corresponding to a light-water density of 1.000 g/cm^3), using the Vanderbilt pseudopotentials, the BLYP functional, and a plane-wave cutoff of 60 Ry. The system was equilibrated for 2 ps, followed by 4 ps of data collection.

2.2. Static DFT Cluster Calculations. Quantum-mechanical geometry optimizations were performed for $Fe(D_2O)_n^{3+}$ high-spin clusters with $n = 4$ and 6, using the BLYP functional and the GAUSSIAN 98 program package.[41] The local basis set employed here was 6-31G**, i.e., a split valence basis, including polarization functions. Corresponding cluster optimizations with the CPMD program package were also carried out, using the same computational parameters as in the simulation of the solution (cubic box with 10.16 Å side length, BLYP functional, ultrasoft pseudopotentials, plane waves with an energy cutoff at 60 Ry), but no periodic boundary conditions. Comparison of the local-basis and the plane-wave (PW) methods allows us to test some aspects of the accuracy of the CPMD electronic structure calculations and gives at least an indication of the reliability of the quantum-mechanical level used in the condensed-matter simulation. In all calculations we have completely optimized the geometries of the ion−water clusters. All interaction energies for the local basis-set calculations were corrected for the basis-set superposition error (BSSE) with the counterpoise method.[42]

An isolated D_2O(g) molecule was also optimized with the BLYP/6-31G** and the BLYP/US-PW methods, using the Gaussian and the CPMD programs, respectively; in the CPMD calculation the same procedure as for the clusters was used.

2.3. Classical MD Simulations. Classical MD simulations ("CLMD" in the following) were performed for two different Fe^{3+}(aq) solutions, namely for (i) one Fe^{3+} ion in 512 D_2O molecules (denoted *CLMD-512* in the following), and (ii) one Fe^{3+} ion in 32 D_2O molecules (*CLMD-32*). The ion−water potential was taken from Curtiss et al.[16] and the water model was a flexible SPC-based model by Amira et al.[43] The classical MD simulations were carried out in the NVT ensemble (temperature close to 300 K at a corresponding light-water density of 1.000 g/cm^3) with the Nosé−Hoover constant temperature control.[44,45] In all cases, the Coulombic interactions in the system were treated by the Ewald lattice summation method,[46] including the charged system term.[47] The side length of the cubic simulation box with periodic boundaries was 24.88 Å for the CLMD-512 simulation and 10.16 Å for the CLMD-32 simulation. Each simulation was equilibrated for about 5 ps and the data collection was 100 ps long, with a time step of 0.5 fs. The atomic coordinates were dumped to disk every time step. The drift of the pseudo-Hamiltonian was for all simulations below 0.1% over the whole run.

A classical MD simulation with the same potentials for a system consisting of one Fe^{3+} ion in 512 non-deuterated H_2O molecules was recently published by us.[22]

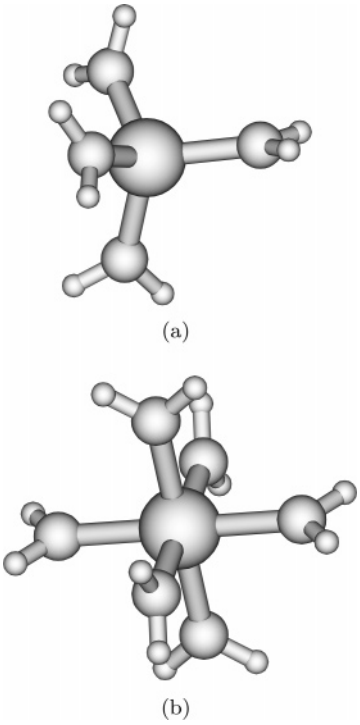

Figure 1. Optimized geometries of the $Fe(D_2O)_n^{3+}$, $n = 4$, 6, clusters, computed at the BLYP/6-31G** level with the Gaussian program (see text).

3. Results and Discussion

3.1. Optimized $Fe(D_2O)_n^{3+}$ Complexes.

As mentioned, we have studied high-spin $Fe(D_2O)_n^{3+}$ complexes, with $n = 4$ and 6, to evaluate the performance of the combination of the Vanderbilt pseudopotential with a plane-wave cutoff of 60 Ry. For a highly charged ion such as Fe^{3+}, the significance of possible charge transfer states is important to consider. Thus for $Al(H_2O)_1^{3+}$, for example, it was shown in the literature[48] that the stable electronic structure at an infinite ion−water distance corresponds to $Al^{2+}(H_2O)^+$. In the present work, the ferric ion was found to form stable hydrates for complexes with more than three water molecules.

In an earlier $Fe(H_2O)_n^{3+}$ ab initio study in the literature by Curtiss et al.,[32] the clusters were not optimized, which makes a direct comparison with their results difficult. However, Chang and Wang[33] performed symmetry-constrained BLYP DFT calculations for the hexaaqua ion, using a "double-numerical quality" local basis set augmented by polarization functions (DNP), which was argued by them to be comparable in size to the 6-31G** basis set. Their results are in modest agreement with our BLYP/6-31G** results.

The optimized geometries of the two complexes are given in Figure 1. The resulting geometries *look* the same with both basis-sets used, and the optimized Fe^{3+}−O distance, the internal geometry of the water molecules, and the total interaction energy are collected in Table 2. First of all we note that the BLYP/6-31G** and the BLYP/US-PW calculations give almost identical optimized geometries, and quite similar interaction energies. The good agreement between the local-basis and the plane-wave results for the ion−water clusters supports the adequacy of using the pseudopotentials and the plane-wave cutoff chosen, and the fully dynamical CPMD simulations of the Fe^{3+}(aq) solution were performed with the same plane-wave method. The validation of this particular plane-wave approach could be extended for instance by testing different combinations of plane-wave cutoffs, pseudopotentials, and functionals. Such an extensive testing procedure, however, is outside the scope of the present paper. We have chosen the Vanderbilt pseudopotentials in combination with the BLYP functional for the CPMD simulations here. This method has been successfully applied in previous studies of aqueous systems; see for instance refs 4 and 49.

TABLE 2: Optimized Geometries and Interaction Energies (in Å, deg, and kcal mol^{-1}) of $Fe(D_2O)_n^{3+}$ ($n = 4$, 6) Clusters[a]

property	method	H_2O(g)	$Fe(D_2O)_4^{3+}$	$Fe(D_2O)_6^{3+}$
$R(Fe^{3+}-O)$	BLYP/US-PW		1.963	2.064
	BLYP/6-31G**		1.961	2.064
r(OD)	BLYP/US-PW	0.976	0.999	0.988
	BLYP/6-31G**	0.976	0.999	0.988
θ(DOD)	BLYP/US-PW	104.4	106.28	106.51
	BLYP/6-31G**	104.4	106.45	106.52
ΔE(tot)/n	BLYP/US-PW		−146.5	−113.7
	BLYP/6-31G**		−151.5	−117.3

[a] The BLYP/US-PW entry refers to calculations with the CPMD program, using Vanderbilt pseudopotentials, the BLYP functional, and a 60 Ry plane-wave cutoff. The BLYP/6-31G** calculations were performed with the Gaussian program. ΔE is E(optimized cluster) − $E(Fe^{3+})$ − E(gas-phase water molecule with cluster geometry). The ΔE values from the Gaussian calculations have been counterpoise corrected.

Further analysis of the structural and energetic results in Table 2 shows that with both the plane-wave and the local-basis methods, the Fe^{3+}−O distance increases and the O−D distance decreases upon addition of two new water molecules to the cluster. The DOD angle opens up slightly with respect to the free water molecule, but seems to be rather insensitive to the increase of the cluster size, as also reported in previous CPMD studies (see, e.g., ref 4). As expected, the binding energy per water molecule is seen to decrease when the cluster size increases. In summary, an increase of the cluster size from 4 to 6 water molecules is seen to have three main effects: (1) the Fe^{3+}−O distance increases by 0.1 Å, (2) the OD distance decreases by 0.01 Å, and (3) the binding energy per water molecule decreases by approximately 20%.

3.2. Classical and Car−Parrinello MD Simulations.

3.2.1. Structural Properties.

(a) Radial Distribution Functions. Ion−oxygen, ion−deuterium, and oxygen−oxygen radial distribution functions (RDFs) were computed for the CPMD-32, CLMD-32, and CLMD-512 simulations and the results are shown in Figure 2 (the oxygen−oxygen RDFs are not shown in the figure).

The most important features are the sharp *first-shell* peak and the well-separated and clearly visible second peak in the Fe−O RDF. The first-peak distances for the different RDFs are listed in Table 3, together with experimental values. Published experimental ion−oxygen distances lie in the range 1.98−2.05 Å (cf. data compilation in refs 1 and 50) and previously published MC and MD simulations give Fe^{3+}−oxygen distances in the range 1.96−2.11 Å.[16−22] The Fe−O maximum in the present study occurs at 1.98 and 1.96 Å, respectively, for the CLMD-32 and CLMD-512 simulations and at 2.06 Å for the CPMD-32 simulation. The first-shell peak maximum at a shorter distance, together with the sharper and higher peak, reflect a more strongly bound first hydration shell for the classical MD results compared to the CPMD simulation. The shorter Fe−O distance in our classical simulations is related to the fact that the empirical pair potential parameters by Curtiss et al. were adjusted to reproduce an experimental Fe−O distance of 1.98 Å (see ref 16).

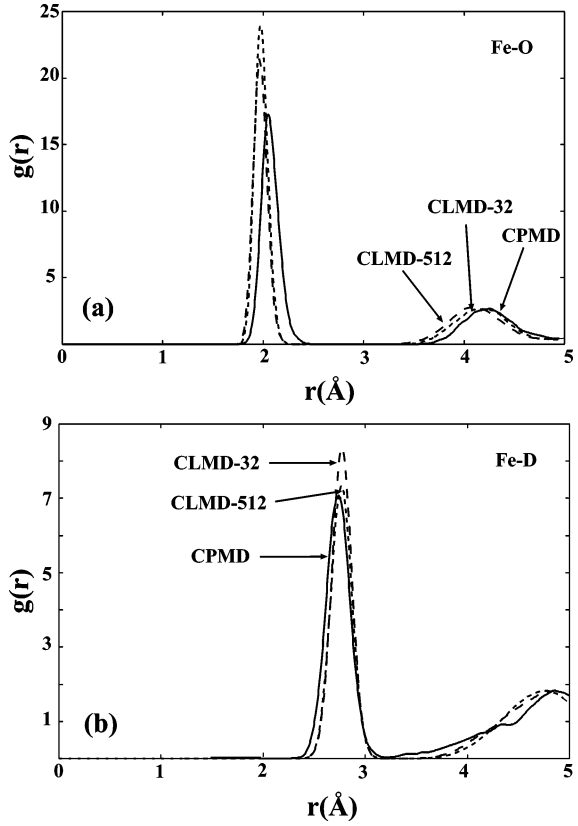

Figure 2. Radial distribution function from the three different simulations: CPMD (full line), CLMD-512 (dashed line), and CLMD-32 (dotted line): (a) Fe^{3+}−O and (b) Fe^{3+}−D.

TABLE 3: Structural Properties for the First and Second Hydration Shells, Calculated from the Different Radial Distribution Functions from the CPMD and the CLMD Simulations[a]

	CPMD-32	CLMD-32	CLMD-512	experiment
first shell				
$R(Fe^{3+}-O)$	2.05	1.98	1.96	1.98−2.05[1,50]
$R(Fe^{3+}-D)$	2.74	2.77	2.76	
second shell				
$R(Fe^{3+}-O)$	4.26	4.14	4.11	
$R(Fe^{3+}-D)$	4.96	4.88	4.76	
between 1st and 2nd shell				
R(O···O)	2.67	2.64	2.63	2.68
ΔR(O···O) wrt $D_2O(l)$	−0.15	−0.10	−0.11	−0.18[51,52]
1st-shell coord no.	6	6	6	6[1,50]
2nd-shell coord no.	11.5	11	12.5	

[a] Experimental literature values derived from diffraction and IR spectroscopy are included (see text). All distances are in Å.

The peak maximum in the Fe−D RDF for the CPMD simulations occurs at a shorter distance (2.74 Å) compared to the classical MD results (2.77 Å) due both to different Fe−O distances and tilt angles (see later) but also to the fact that the optimized O−H bond length (r_e) of an isolated water molecule with this US-PW method is shorter (0.976 Å) (and closer to experiment at 0.957 Å) than that of the SPC water model (1.00 Å). As for the difference between the CLMD-32 and the CLMD-512 simulations, we note that the slightly higher first-shell peak in the ion−oxygen RDF for the CLMD-32 simulation demonstrates that the small box-size leads to a slightly over-structured system.

The main feature of the O···O RDF calculated *between the water molecules in the first and second hydration shells* (not shown here) is a sharp peak with a maximum at 2.64 Å for the two classical simulations and 2.67 Å for the CPMD simulation. The height of the peak is 18.3, 23.9, and 21.4, respectively. This O···O distance is significantly shorter than the corresponding average O···O distance in liquid water, which is 2.74 Å for the SPC+CCL water model and 2.82 Å for the CPMD simulations, i.e., shortenings of 0.10 and 0.15 Å, respectively, have occurred. Incidentally, the ion···water···water cooperativity is also reflected in the Fe−O distance, which has decreased by ∼0.02 Å in the CPMD simulations compared to the isolated $Fe(D_2O)_6^{3+}$ BLYP/US-PW complex in Table 2. Experimentally, for some other trivalent ions, namely for both Al^{3+}(aq) and Cr^{3+}(aq), the shortening of the O···O distance between the first and second hydration shells was reported to be 0.18 Å (compared to a value of 2.86 Å for pure liquid water[51]), using the IR-measured frequency at the OH stretching band maximum for water molecules in the first hydration shell[52] and a ν(OH) vs R(O···O) correlation curve constructed by Berglund et al.[53] from IR data and neutron diffraction data for crystalline hydrates. For our classical simulations, the shortening thus appears to be too small compared to experiment, probably because the cooperative ion−water (first shell)···water (second shell) polarizations present in a real ionic solution were not included in the model. The CPMD simulation for Fe^{3+}(aq) reproduces these experimental results significantly better, since here the many-body ion−hydration shell interactions are taken into account for all water molecules. However, in their CPMD study of Mg^{2+}, Lightstone et al. observed an O···O distance shortening of only 0.03 Å compared to the bulk[8] (IR data from the Lindgren group suggest a shortening of 0.08 Å[51]). Significant shortenings of the O···O distances were also found by us in recent classical MD simulations of Mg^{2+}(aq) and Al^{3+}(aq), using a polarizable water model.[54] For Mg^{2+} the calculated shortening was 0.09 Å, and for Al^{3+} it was 0.20 Å.

We can conclude that the distance between the oxygen atoms in the first and second hydration shells is very sensitive to the inclusion of the many-body effects beyond the first hydration sphere.

The ion−oxygen and ion−deuterium RDFs in Figure 2 show a clearly visible second maximum, corresponding to *the second hydration shell*. The ion−water distances for the second-shell maximum are also listed in Table 3. The most important feature here is the significantly longer ion−second hydration shell distance in the case of the CPMD simulation. For the classical simulations we obtain distances of 4.11 and 4.14 Å for the CLMD-512 and CLMD-32 simulations, respectively, whereas for the CPMD we find a distance of 4.26 Å. This large difference in ion−second shell distance is mainly a consequence of the fact that we compare results from two different methods, each with its own set of systematic errors (CPMD and CLMD); the longer ion−second shell distance for CPMD is consistent with the fact that both the ion−first shell and the first shell···second shell distances are longer for CPMD, as discussed above. Longer ion−second shell distances have also been observed in classical simulations by using a polarizable water model, see for instance ref 54.

The second hydration shell lies at the edge of the box and we see that the small box size causes a small shift to longer distances (0.03 Å) of the second hydration shell peak for the simulation with 32 water molecules compared to the box with 512 water molecules.

(*b*) *The Tilt of the Water Molecules in the First and Second Hydration Shells.* The first hydration shell around the ferric ion contains on average 6 water molecules in an octahedral arrangement for all three simulations. The second hydration shell has a broader distribution of (instantaneous) coordination

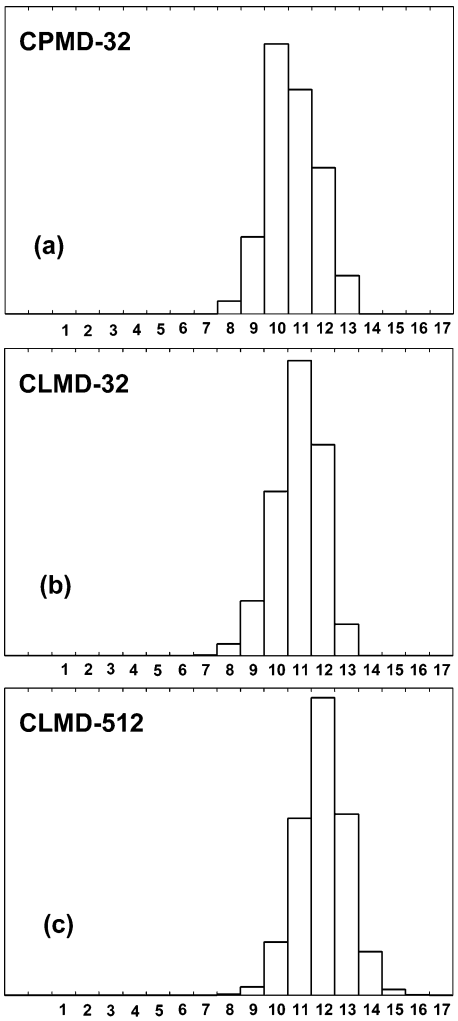

Figure 3. Distribution of the coordination number in the second hydration shell of Fe^{3+} for the three different simulations: (a) CPMD-32, (b) CLMD-32, and (c) CLMD-512.

numbers, as seen in Figure 3, with values in the range 8−13 for the CLMD-32 simulations, and even broader for the CLMD-512 simulation. The average coordination number for the second shell is 11.5 for CPMD-32, 11.0 for CLMD-32, and 12.5 for CLMD-512, as obtained from integration of the radial distribution function up to the point where it becomes 1 after the second shell. This clearly shows that the system-size effect is an important issue to consider when results from classical and CPMD simulations are compared.

Here, the orientations of first-shell and second-shell water molecules around the ion have been calculated in terms of angular-radial distribution functions, namely the distribution of the tilt angle as a function of the distance from the ion. The tilt angle θ_{dihed} is here defined as the dihedral angle ion−H'_1−H'_2−O', where H'_1, H'_2, and O' correspond to the positions of a translated water molecule, as shown in Figure 4 (for an elaborate discussion on the advantages of this dihedral angle as a measure of the tilt angle, see ref 54). Other studies which include an analysis of angular-radial distribution functions have for instance been presented by Svishchev and Kusalik,[55] Degrève and Quintale,[56] and Spångberg and Hermansson.[54,57]

Figure 5 shows the two-dimensional angular-radial distribution functions (θ_{dihed}, r) for the CPMD-32, CLMD-32, and CLMD-512 simulations as contour maps. The average tilt angles in the first and second shells are collected in Table 4 as 180° − $\langle\theta_{\text{dihed}}\rangle$, to make the comparison with the literature results easier.

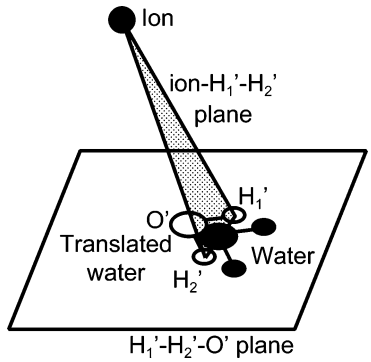

Figure 4. Definition of the dihedral angle as the angle between the plane of the water molecule and a plane containing the ion and the two hydrogen atoms in a translated water molecule; see text for details.

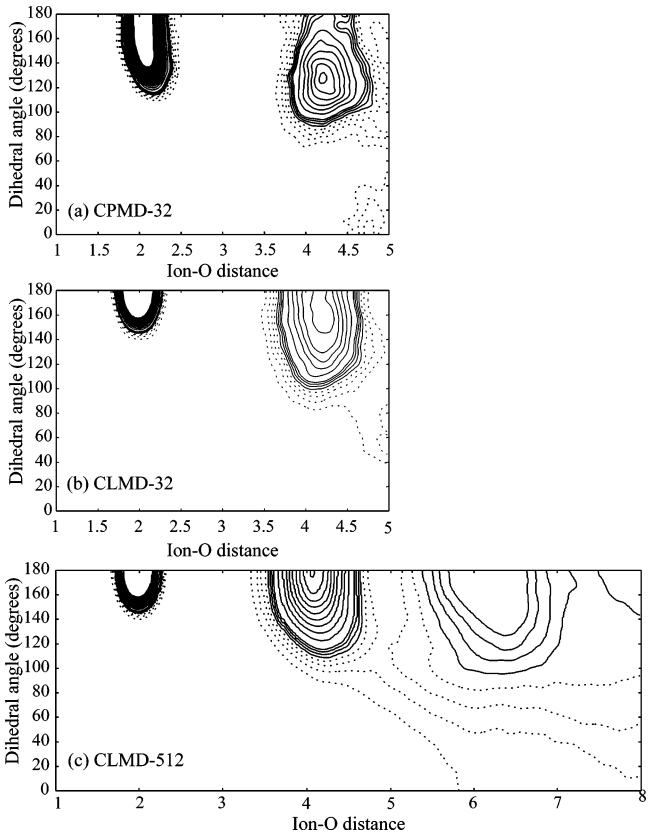

Figure 5. Contour plots of the angular-radial distribution function for (a) the CPMD-32 simulation, (b) the CLMD-32 simulation, and (c) the CLMD-512 simulation. The *x* axes show the distance between the ion and the water oxygen, the *y* axes show θ_{dihed} (see text). Contour levels: larger than 1 (solid), 1 and smaller (dashed). The interval between the contour levels is 0.25 for values smaller than 2, and 1 for values larger than 2.

For the first hydration shell, we obtain maxima for θ_{dihed} at about 180°, corresponding to a trigonal coordination, i.e., a situation where the ion, the oxygen, and the two hydrogen atoms of the water molecule lie in the same plane. The CPMD simulation yields a more flexible first hydration shell, and more tilted water molecules and hence a significantly broader distribution. The two classical simulations exhibit essentially the same narrow distribution of θ_{dihed} close to 180° for the first shell, but the average tilt angle for the two classical simulations differs by about 10° and the distribution is broader for the small box size. Previous classical MD work for Fe^{3+}(aq) reports a value of 7.7° for the tilt of the first shell water molecules,[18] while experimental studies[58,59] report two different tilt angles, 20° and 40°, although

TABLE 4: Average Tilt Angles for the Water Molecules in the First and Second Hydration Shells, Computed as $180° - \langle\theta_{dihed}\rangle$ from the Three Simulations[a]

	$180° - \langle\theta_{dihed}\rangle$	
	1st shell	2nd shell
CPMD-32	23	55
CLMD-32	9	39
CLMD-512	8	30
MD[18] [b]	8[c]	
neutron diffraction[58,59]	20, 40[d]	

[a] The θ_{dihed} angle is defined in Figure 4 and discussed in the text. A value of zero for $180° - \langle\theta_{dihed}\rangle$ corresponds to a planar, trigonal orientation. [b] MD simulation with 100 water molecules and an Fe^{3+}–water potential based on the potential by Curtiss et al.[16] [c] The tilt angle was here defined as the angle between the Fe–O vector and the HOH bisector. [d] The tilt angle was here calculated from the radial distribution functions.

it must be borne in mind that slightly different definitions for the tilt angle were used in the different cases.

The second-shell water molecules are more tilted in the angular CPMD simulation while the width of the angular distribution is similar to that of the classical simulations. No important size dependence can be seen in the contour plots for the CLMD-32 and the CLMD-512 simulations. The most apparent difference between the classical and CPMD simulations is found in the region of the small θ_{dihed} angles (between 0° and 90°), corresponding to a situation where the hydrogen atoms of the water molecules point toward the ion. This region has a significant probability density only for the CPMD simulation. Similar orientations for the second shell water molecules have been obtained for the CPMD simulations of the hydration shell around Li^+,[3] Na^+,[7] and Mg^{2+},[8] as well as for classical MD simulations for Li^+, Na^+, Mg^{2+}, and Al^{3+}.[54] This means that the influence of the ferric ion on the water orientations and the hydrogen-bond pattern is not as strong for the CPMD simulations as for the force-field CLMD simulations.

In summary, we find for the first hydration shell that the tilt angle does not depend very much on system size: there is almost no difference between the CLMD-32 and the CLMD-512 simulations. For the second shell, more tilted water molecules and a broader angular distribution were observed for the smaller box, because these water molecules lie close to the "edge" of the box and are more influenced by the periodic image of the metal ion. For the CPMD simulations, we find a more flexible first hydration shell and fewer water molecules and a greater variety of bonding patterns in the second hydration shell, compared to the classical MD simulations.

3.2.2. Intramolecular Vibrations.

(a) Intramolecular Geometry. OD vibrational shifts are closely related to the distortion of the intramolecular geometry. Thus, before we move on to discussing the calculation of OD vibrational spectra, we first discuss the average water geometry resulting from the simulations. The Fe^{3+} ion strongly distorts the surrounding water molecules. Experimental[60] and ab initio (see, for example, ref 61) studies in the crystalline state show that the OH bonds of the water molecules surrounding a cation are significantly elongated compared to those of the isolated water molecule. A lengthening of the OH bond as well as a closing of the HOH angle has also been observed in previous MD simulations of aqueous solutions.[62,63]

In the current study, the average O–D bond lengths and DOD angles for the water molecules in the first hydration shell around Fe^{3+} and for pure water are listed in Table 5. No significant dependence on the system size is found for the intramolecular

TABLE 5: Intramolecular Geometry (in Å and deg) of the Water Molecule As Obtained from the CPMD-32 and CLMD-32 Simulations, Compared to Experiment[a]

	CPMD-32	CLMD-32	CLMD-512	experiment
r(OD)				
D_2O(g)	0.98	1.00	1.00	0.9572[70] [b]
D_2O(l)	0.99	1.01	1.01	
Fe^{3+}(aq), 1st shell	1.01	1.06	1.06	1.02[64] [c]
θ(DOD)				
D_2O(g)	105.2	109.5	109.5	104.52[70]
D_2O(l)	105.7	105.1	105.1	[d]
Fe^{3+}(aq), 1st shell	107.0	98.8	99.0	[d]

[a] The experimental values are further discussed in the text. [b] Derived from a rotation–vibration spectrum. [c] From NMR experiment for $Al(H_2O)_6^{3+}$ in aqueous solution. [d] Neutron diffraction data from crystalline hydrates suggest an opening of the angle with respect to the gas-phase value.[60]

water geometries. We find that for the classical MD and the CPMD simulations, the OD bond length in the first hydration shell increases by 0.05 and 0.02 Å, respectively, compared to pure liquid water. These shifts are in overall agreement with the experimentally observed OH bond-length increase for the first-shell water molecules around Al^{3+} in aqueous solution (r_{OH} = 1.019 Å, as determined by NMR)[64] compared to the liquid water value (r_{OH} = 0.96 Å, as determined by neutron diffraction).[65] It should be noted, however, that the experimental value 0.96 Å appears to be quite uncertain, i.e., slightly erroneous, since the OH distance for the water molecule in the gas phase has been determined to be 0.971 Å (equilibrium structure with zero-point vibrational correction)[66] and the bond in the liquid phase is definitely expected to be elongated with respect to the gas phase. Previous classical MD simulations of $AlCl_3$(aq) found an OH bond-length increase for the water molecules in the first hydration shell of 0.07 Å.[63] Other simulations, of the QM/MM type, on the other hand, have yielded a shortening of the first-shell OH bonds with respect to pure liquid water;[30] that result appears nonphysical, however, since the strong field from the trivalent ion should be expected to give rise to an OH bond lengthening.

The bond angles change considerably for the water molecules in the first hydration sphere. For the classical MD simulations, the water angle is seen to decrease by 11°, compared to the free-water angle. Such a large closing of the water angle is in contrast to the situation in ionic crystalline hydrates,[60] where (on average) an opening of the HOH angle was found in a large compilation of neutron diffraction studies, with very few examples of such a large angle decrease as 10°. This discrepancy between our results for the flexible SPC+CCL water model and experiment reflects what seems to be a common problem for flexible water models and has been discussed before in the literature.[67,68] To the best of our knowledge, only the flexible water model by Burnham and Xantheas[68] shows an opening of the HOH angle in the gas-to-liquid transfer. For the CPMD simulations we here obtain an increase of the DOD water angle by 1.8° compared to that of the free water molecule. This value is very similar to "typical" values found for the water molecules in ionic crystalline hydrates. Larger HOH angles have also been reported for the first-shell water molecules around Be^{2+}, using CPMD,[4] and around Fe^{3+}, using the QM/MM method.[30] Also the cluster calculation in section 3.1 showed an increase in the water angle due to the cation.

In conclusion, both the classical MD and the CPMD simulations reproduce the lengthening of the O–D bond, while the opening of the DOD angle is only present in the CPMD simulation.

TABLE 6: Positions of the Peak Maxima of the OD Stretching Bands (in cm^{-1}) Calculated for the Water Molecules in the First Hydration Shell of Fe^{3+} from the CPMD-32 and CLMD-32 Simulations[a]

	CPMD-32		CLMD-32		CLMD-512		experiment	
	"ω"	"$\Delta\omega$"	"ω"	"$\Delta\omega$"	"ω"	"$\Delta\omega$"	ν	$\Delta\nu$
D_2O(g)	2695[b]		2825[c]		2825[c]		2727[70]	
D_2O(l)	2340	−355	2590	−235			2503[69]	−225
Fe^{3+}(aq), 1st shell	2160	−535	2330	−495	2290	−535	2200[52]	−525

[a] The frequency shifts are given with respect to the isolated gas-phase molecule. The frequencies obtained from the Velocity Autocorrelation Function are denoted "ω" because that method generates essentially harmonic OD frequencies (see text). All the numbers in the table have been rounded off to end with 0 or 5. [b] Harmonic frequency of a single optimized D_2O(g) molecule (see section 2.2), calculated by finite differences of the first derivatives. [c] Harmonic frequency of the CCL potential.

(*b*) *Vibrational Spectra.* The presence of multivalent metal cations in aqueous solutions results in downshifts of the OD vibrational frequency of the surrounding water molecules, as observed by infrared and Raman spectroscopic measurements. Vibrational spectroscopy is one of the most sensitive experimental methods to study ion−solvent interaction. For liquid D_2O, the peak maximum of the experimental OD stretching band falls at 2503 cm^{-1},[69] downshifted by ca. 220 cm^{-1} compared to the average value of the antisymmetric and the symmetric OD vibrations in the gas-phase D_2O molecule (2727 cm^{-1}).[70] For Fe^{3+}(aq), no infrared or Raman spectroscopic data for the first-shell OH and OD stretching vibrations are available, but experimental results for other trivalent cations, such as Al^{3+}, Cr^{3+}, and Rh^{3+}, have been derived by the so-called double-difference method by Lindgren and co-workers.[52] The experimental IR spectra for water molecules in the first hydration spheres around those three ions show OD bands centered around 2200 cm^{-1}, i.e., downshifted by ∼525 cm^{-1} with respect to the average gas-phase frequency. In the following, the reliability of the absolute and relative frequencies calculated for Fe^{3+}(aq) from the CPMD simulations will be assessed by comparison with the classical MD results as well as with the experimental data for the three trivalent ions from ref 52.

The vibrational frequencies presented were computed from the Fourier transform of the velocity autocorrelation function for the relative velocities of the D atoms with respect to the velocity of the O atom, unless stated otherwise. When comparing the calculated frequencies with the experimental results, it is important of keep in mind that for both the classical and the CPMD simulations the motion of the atoms is treated classically and thus only the bottom part of the stretching potential (close to r_e(OD)) is sampled. This means that our simulations yield very close to harmonic stretching frequencies, while experiment yields the anharmonic stretching frequency (see, for example, ref 61).

The OD stretching frequencies for the water molecules in the gas phase, in pure liquid D_2O, and in the first hydration sphere of the Fe^{3+} ion are listed in Table 6. The spectra calculated from the CPMD simulations for pure liquid water and for the first-shell water molecules around the ion are shown in Figure 6. The *gas-phase OD stretching frequency* from the classical MD simulation is 2825 cm^{-1}, very close to the experimental harmonic value (2826 cm^{-1}),[70] since the intramolecular part of the classical SPC+CCL potential indeed *is* the experimental gas-phase water potential. The CPMD simulation, however, yields a harmonic gas-phase frequency at 2696 cm^{-1}, approximately 130 cm^{-1} lower than experiment. For *pure liquid water*, the OD frequency lies at 2590 cm^{-1} for the classical MD and at 2340 cm^{-1} for the CPMD. The experimental gas-to-liquid downshift of 225 cm^{-1} is thus well reproduced for the classical simulations: we find a downshift of 240 cm^{-1}. For the CPMD simulation, the gas-to-liquid shift is 355 cm^{-1}, about 120 cm^{-1} too large.

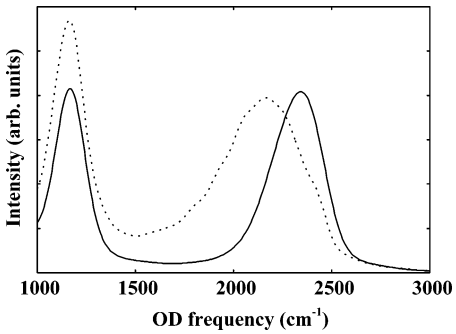

Figure 6. The calculated vibrational spectrum from the CPMD simulations in the bending and stretching mode region of D_2O for pure D_2O (solid line) and in the first shell around Fe^{3+} (dotted line), obtained from the Fourier transform of the velocity autocorrelation functions.

In *the simulated Fe^{3+}(aq) solutions*, the water molecules around the ferric ion are much more downshifted than in the pure liquid. The simulated spectrum for the first-shell water molecules around Fe^{3+} has a maximum at 2340 cm^{-1} for the CLMD-32 simulation and 2160 cm^{-1} for the CPMD. The CLMD-512 yields a peak at 2290 cm^{-1}, i.e., the small system size shifts the OD frequency upwards by about 40 cm^{-1}. The first-shell OD stretching band is thus downshifted by 500 (CLMD-32), 535 (CLMD-512), and 535 cm^{-1} (CPMD) with respect to the gas-phase frequency, and by 260 (CLMD-32), 300 (CLMD-512), and 180 cm^{-1} (CPMD) with respect to the pure liquid water frequency.

We conclude that the classical simulations, with the set of potentials selected here, perform well for the gas phase, as well as for the pure liquid and the Fe^{3+}(aq) solution; in all cases both good absolute frequencies and good frequency downshifts are obtained. The CPMD calculations give too low an absolute gas-phase frequency and the gas-to-pure liquid shift is not well reproduced; it is 130 cm^{-1} too large. On the other hand, the frequency downshift for the first-shell hydration waters with respect to pure D_2O(l) is about 120 cm^{-1} too small. The small system size contributes to the too small downshift.

4. Conclusions

In this work we have performed static CPMD geometry optimizations of small $Fe^{3+}(D_2O)_n$ clusters, with $n = 4$ and 6, and CPMD simulations at room temperature for the hydration shell of a single Fe^{3+} ion in a periodic box with 32 water molecules (a model of an aqueous solution). The cluster calculations were compared with local-basis quantum-mechanical calculations to make some assessment of the quality of the electronic structure calculations in the CPMD method. The solution simulations were compared with classical MD simulations containing 32 water molecules and 512 water molecules to make some assessment of the influence of the system size and interaction model on the calculated solution properties. For the structural properties of the solution, we obtain results in good agreement with experiment for both the classical MD and the CPMD simulations. Here, the major difference between the classical and CPMD description is found in the distance between the first and the second hydration shells. For this property a sound description of the many-body effects is crucial in order to find values close to experiment.

We have also analyzed the angular distribution of the water molecules in the first and second shells. The CPMD results indicate a more flexible first hydration shell compared to CLMD. The second-shell coordination number is lower in the CPMD simulations and there exist second-shell water molecules with their hydrogen atoms pointing toward the ion in the CPMD simulations. For the second shell, the CLMD simulations show a clear size effect: for the small system, a much broader angular distribution was observed. This is because the water molecules close to the edge of the box (assuming the ion is in the middle) are perturbed by the ion's periodic images.

For the intramolecular vibrations we conclude the following. The combination of the SPC+CCL flexible-water model with the Curtiss ion−water potential returns both good absolute OD stretching frequencies and frequency shifts. From the CPMD calculations we obtain less convincing results. We obtain a too low absolute gas-phase frequency and the experimental gas-to-pure liquid shift is not well reproduced (too large by some 130 cm^{-1}). Also the frequency downshift of the water molecules in the first hydration shell with respect to pure $D_2O(l)$ is not well reproduced (too small by some 120 cm^{-1} compared to experiment).

Several factors can be responsible for discrepancies observed between experimental and CPMD-calculated OD frequencies. Inconsistencies in the harmonic/anharmonic vibrational description between experiment and calculation, and the limited system size in the CPMD simulations are two factors which have been addressed in the present study. Remaining discrepancies could arise from the choice of the exchange-correlation functional, the pseudopotential, and the fictitious electron mass in the CPMD simulations.

Acknowledgment. This work has been supported by the Swedish Research Council (VR) and the European FP5 IHP program (Research Training Network Contract No. HPRN-CT-2000-19).

References and Notes

(1) Ohtaki, H.; Radnai, T. *Chem. Rev.* **1993**, *93*, 1157.
(2) Car, R.; Parrinello, M. *Phys. Rev. Lett.* **1985**, *55*, 2471.
(3) Lyubartsev, A. P.; Laasonen, K.; Laaksonen, A. *J. Chem. Phys.* **2001**, *114*, 3120.
(4) Marx, D.; Sprik, M.; Parrinello, M. *Chem. Phys. Lett.* **1997**, *273*, 360.
(5) Ramaniah, L.; Bernasconi, M.; Parrinello, M. *J. Chem. Phys.* **1998**, *109*, 6839.
(6) Vuilleumier, R.; Sprik, M. *J. Chem. Phys.* **2001**, *115*, 3454.
(7) White, J. A.; Schwegler, E.; Galli, G.; Gygi, F. *J. Chem. Phys.* **2000**, *113*, 4668.
(8) Lightstone, F. C.; Schwegler, E.; Hood, R. Q.; Gygi, F.; Galli, G. *Chem. Phys. Lett.* **2001**, *343*, 549.
(9) Lubin, M. I.; Bylaska, E. J.; Weare, J. H. *Chem. Phys. Lett.* **2000**, *322*, 447.
(10) Ramaniah, L.; Bernasconi, M.; Parrinello, M. *J. Chem. Phys.* **1999**, *111*, 1587.
(11) Bakó, I.; Hutter, J.; Pálinkás, G. *J. Chem. Phys.* **2002**, *117*, 9838.
(12) Ensing, B.; Baerends, E. J. *J. Phys. Chem. A* **2002**, *106*, 7902.
(13) Ensing, B.; Buda, F.; Blöchl, P. E.; Baerends, E. J. *Phys. Chem. Chem. Phys.* **2002**, *4*, 3619.
(14) Pasquarello, A.; Petri, I.; Salmon, P. S.; Parisel, O.; Car, R.; Tóth, E.; Powell, D. H.; Fischer, H. E.; Helm, L.; Merbach, A. E. *Science* **2001**, *291*, 856.
(15) Raugei, S.; Klein, M. L. *J. Chem. Phys.* **2002**, *116*, 196.
(16) Curtiss, L. A.; Halley, J. W.; Hautman, J.; Rahman, A. *J. Chem. Phys.* **1987**, *86*, 2319.
(17) Floris, F.; Persico, M.; Tani, A.; Tomasi, J. *Chem. Phys. Lett.* **1992**, *199*, 518.
(18) Kneifel, C. L.; Friedman, H.; Newton, M. D. *Z. Naturforsch.* **1989**, *44a*, 385.
(19) Kneifel, C. L.; Newton, M. D.; Friedman, H. L. *J. Mol. Liq.* **1994**, *60*, 107.
(20) Degrève, L.; Quintale, C., Jr. *J. Electroanal. Chem.* **1996**, *409*, 25.
(21) Guàrdia, E.; Padró, J. A. *Chem. Phys.* **1990**, *144*, 353.
(22) Amira, S.; Spångberg, D.; Hermansson, K. *J. Phys. Chem. B* **2004**, *108*, 496.
(23) Rustad, J. R.; Hay, B. P.; Halley, J. W. *J. Chem. Phys.* **1995**, *102*, 427.
(24) González-Lafont, A.; Llunch, J. M.; Oliva, A.; Bertrán, J. *J. Comput. Chem.* **1991**, *12*, 1165.
(25) Friedman, H. L.; Newton, M. D. *J. Electrochem. Soc.* **1987**, *134*, 138.
(26) Kuharski, R. A.; Bader, J. S.; Chandler, D.; Sprik, M.; Klein, M. L.; Impey, R. W. *J. Chem. Phys.* **1989**, *89*, 3248.
(27) Bader, J. S.; Chandler, D. *J. Phys. Chem.* **1992**, *96*, 6423.
(28) Kumar, P. V.; Tembe, B. L. *J. Chem. Phys.* **1992**, *97*, 4356.
(29) Babu, C. S.; Madhusoodanan, M.; Sridhar, G.; Tembe, B. L. *J. Am. Chem. Soc.* **1997**, *119*, 5679.
(30) Remsungnen, T.; Rode, B. M. *Chem. Phys. Lett.* **2003**, *367*, 586.
(31) Remsungnen, T.; Rode, B. M. *J. Phys. Chem. A* **2003**, *107*, 2324.
(32) Curtiss, L. A.; Halley, J. W.; Hautman, J. *Chem. Phys.* **1989**, *133*, 89.
(33) Chang, C. M.; Wang, M. K. *Chem. Phys. Lett.* **1998**, *286*, 46.
(34) Becke, A. D. *Phys. Rev. A* **1988**, *38*, 3098.
(35) Lee, C.; Yang, W.; Parr, R. C. *Phys. Rev. B* **1988**, *37*, 785.
(36) Vanderbilt, D. *Phys. Rev. B* **1990**, *41*, 7892.
(37) Louie, S. G.; Froyen, S.; Cohen, M. L. *Phys. Rev. B* **1982**, *26*, 1738.
(38) *CPMD*, Version 3.7.3, Hutter, J. et al.; Max-Planck-Institut für Festkörperforschung and IBM Zurich Research Laboratory, 1995−1999.
(39) Laasonen, K.; Sprik, M.; Parrinello, M. *J. Chem. Phys.* **1993**, *99*, 9080.
(40) Martyna, G. J.; Klein, M. L.; Tuckerman, M. E. *J. Chem. Phys.* **1992**, *97*, 2635.
(41) *GAUSSIAN98*, Frisch, M. J. et al.; Gaussian, Inc.: Pittsburgh, PA, 1998.
(42) Boys, S. F.; Bernardi, F. *Mol. Phys.* **1970**, *19*, 553.
(43) Amira, S.; Spångberg, D.; Hermansson, K. *Chem. Phys.* **2004**, *303*, 327.
(44) Nosé, S. *Mol. Phys.* **1984**, *52*, 255.
(45) Hoover, W. G. *Phys. Rev. A* **1985**, *31*, 1695.
(46) Allen, M. P.; Tildesley, D. J. *Computer Simulations of Liquids*; Clarendon Press: Oxford, UK, 1987.
(47) Hummer, G.; Pratt, L. R.; García, A. E. *J. Phys. Chem.* **1996**, *100*, 1206.
(48) Wasserman, E.; Rustad, J. R.; Xantheas, S. S. *J. Chem. Phys.* **1997**, *106*, 9769.
(49) Sprik, M.; Hutter, J.; Parrinello, M. *J. Chem. Phys.* **1996**, *105*, 1142.
(50) Brunschwig, B. S.; Creutz, C.; Macartney, D. H.; Sham, T. K.; Sutin, N. *Faraday Discuss. Chem. Soc.* **1982**, *74*, 113.
(51) Kristiansson, O.; Eriksson, A.; Lindgren, J. *Acta Chem. Scand.* **1984**, *A38*, 613.
(52) Bergström, P.-Å.; Lindgren, J.; Read, M.; Sandström, M. *J. Phys. Chem.* **1991**, *95*, 7650.
(53) Berglund, B.; Lindgren, J.; Tegenfeldt, J. *J. Mol. Struct* **1978**, *43*, 169.
(54) Spångberg, D.; Hermansson, K. *J. Chem. Phys.* **2004**, *120*, 4829.
(55) Svishchev, I. M.; Kusalik, P. G. *J. Chem. Phys.* **1993**, *99*, 3049.
(56) Degrève, L.; Quintale, C., Jr. *J. Chem. Phys.* **1994**, *101*, 2319.
(57) Spångberg, D.; Hermansson, K. *Chem. Phys.* **2004**, *300*, 165.
(58) Herdman, G. J.; Neilson, G. W. *J. Phys.*: *Condens. Matter* **1992**, *4*, 649.
(59) Herdman, G. J.; Neilson, G. W. *J. Phys.*: *Condens. Matter* **1992**, *4*, 627.
(60) Chiari, G.; Ferraris, G. *Acta Crystallogr. B* **1982**, *38*, 2331.
(61) Ojamäe, L.; Hermansson, K. *J. Chem. Phys.* **1992**, *96*, 9035.
(62) Probst, M. M.; Spohr, E.; Heinzinger, K. *Mol. Simul.* **1991**, *7*, 43.
(63) Lauenstein, A.; Hermansson, K.; Lindgren, J.; Probst, M.; Bopp, P. *Int. J. Quantum Chem.* **2000**, *80*, 892.
(64) van der Maarel, J. R. C.; de Boer, H. R. W.; de Bleijser, J.; Bedeaux, D.; Leyte, J. C. *J. Chem. Phys.* **1987**, *86*, 3373.
(65) Soper, A. K. *Chem. Phys.* **2000**, *258*, 121.
(66) Kuchitsu, K.; Bartell, L. S. *J. Chem. Phys.* **1962**, *36*, 2460.
(67) Stern, H. A.; Berne, B. J. *J. Chem. Phys.* **2001**, *115*, 7622.
(68) Burnham, C. J.; Xantheas, S. S. *J. Chem. Phys.* **2002**, *116*, 5115.
(69) Wyss, H. R.; Falk, M. *Can. J. Chem.* **1970**, *48*, 607.
(70) Benedict, W. S.; Gailar, N.; Plyler, E. K. *J. Chem. Phys.* **1956**, *24*, 1139.